

RESEARCH PAPER

Receptors involved in the modulation of guinea pig urinary bladder motility by prostaglandin D₂

Na N Guan¹, Karl Svennersten², Petra J de Verdier^{2*}, N Peter Wiklund² and Lars E Gustafsson¹

Departments of ¹Physiology and Pharmacology, ²Molecular Medicine and Surgery, Karolinska Institutet, Stockholm, Sweden

Correspondence

Professor Lars E. Gustafsson,
Department of Physiology and
Pharmacology, Karolinska
Institutet, Stockholm S-171 77,
Sweden. E-mail:
lars.gustafsson@ki.se.

*Present address: Department of
Laboratory Medicine, Karolinska
Institutet at Karolinska University
Hospital Huddinge, Stockholm
14186, Sweden

Received

2 October 2014

Revised

17 April 2015

Accepted

22 April 2015

BACKGROUND AND PURPOSE

We have described a urothelium-dependent release of PGD₂-like activity which had inhibitory effects on the motility of guinea pig urinary bladder. Here, we have pharmacologically characterized the receptors involved and localized the sites of PGD₂ formation and of its receptors.

EXPERIMENTAL APPROACH

In the presence of selective DP and TP receptor antagonists alone or combined, PGD₂ was applied to urothelium-denuded diclofenac-treated urinary bladder strips mounted in organ baths. Antibodies against PGD₂ synthase and DP₁ receptors were used with Western blots and for histochemistry.

KEY RESULTS

PGD₂ inhibited nerve stimulation -induced contractions in strips of guinea pig urinary bladder with estimated pIC₅₀ of 7.55 ± 0.15 (*n* = 13), an effect blocked by the DP₁ receptor antagonist BW-A868C. After blockade of DP₁ receptors, PGD₂ enhanced the contractions, an effect abolished by the TP receptor antagonist SQ-29548. Histochemistry revealed strong immunoreactivity for PGD synthase in the urothelium/suburothelium with strongest reaction in the suburothelium. Immunoreactive DP₁ receptors were found in the smooth muscle of the bladder wall with a dominant localization to smooth muscle membranes.

CONCLUSIONS AND IMPLICATIONS

In guinea pig urinary bladder, the main effect of PGD₂ is an inhibitory action via DP₁ receptors localized to the smooth muscle, but an excitatory effect via TP receptors can also be evoked. The urothelium with its suburothelium might signal to the smooth muscle which is rich in PGD₂ receptors of the DP₁ type. The results are important for our understanding of regulation of bladder motility.

Abbreviations

EFS, electrical field stimulation; OAB, overactive bladder syndrome; PGDS, PGD synthase

Tables of Links

TARGETS
GPCRs
DP1 receptor
DP2 receptor
TP receptor

LIGANDS
BW-245C
Diclofenac
PGD ₂
SQ-29548

These Tables list key protein targets and ligands in this article which are hyperlinked to corresponding entries in <http://www.guidetopharmacology.org>, the common portal for data from the IUPHAR/BPS Guide to PHARMACOLOGY (Pawson *et al.*, 2014) and are permanently archived in the Concise Guide to PHARMACOLOGY 2013/14 (Alexander *et al.*, 2013).

Introduction

The PGs have been suggested as modulators of urinary bladder motility for decades. Production of PGs locally within the bladder smooth muscle and mucosa in human and other species has been reported (Abrams *et al.*, 1979; Jeremy *et al.*, 1987). Their production can become pathological in conditions such as bladder outlet obstruction (Masick *et al.*, 2001), spinal cord injury-induced bladder overactivity (Masunaga *et al.*, 2006), inflammation (Wheeler *et al.*, 2001), physical stretch and nerve stimulation. It is well accepted that PG E, F series and T_x act as stimulative modulators to contract the bladder strips and increase the spontaneous activities during *in vitro* experiments in human tissues (Andersson *et al.*, 1977; Palea *et al.*, 1998). *In vivo* urodynamic tests showed increased detrusor pressure and reduced bladder capacity after intravesical administration of PGE₂ (Ishizuka *et al.*, 1995). Intravesical administration of PGE₂ or sulprostone to healthy women resulted in reduced bladder capacity (Schüssler, 1990). There are little data concerning the effect of PGD₂ and receptors involved in the urinary bladder (Rahnama'i *et al.*, 2012). One human study suggested PGD₂ had a low potency to contract the normal bladder strips (Palea *et al.*, 1998). We recently found that PGE₂ and PGD₂ were released mainly from urothelium in guinea pig urinary bladders and that PGD₂ inhibited the motility of guinea pig urinary bladder, induced by nerve stimulation, ACh or ATP (Guan *et al.*, 2014).

There are nine prostanoid receptors classified as: DP₁, DP₂ (CRTH2), EP₁, EP₂, EP₃, EP₄, FP, IP and TP, which are preferentially activated by the major prostanoids PGD₂, PGE₂, PGF_{2α}, PGI₂ and TxA₂ (Woodward *et al.*, 2011). In the respiratory system, PGD₂ exerts its biological effects via DP₁ and DP₂ receptors and can also activate TP receptors (Pettipher *et al.*, 2007; Larsson *et al.*, 2011), but it is not known which receptors are involved in PGD₂ action in the urinary bladder.

Building on the earlier findings that PGE₂ and PGD₂ were released from healthy guinea pig urinary bladder and with the availability of selective DP receptor antagonists, we designed the present study to answer two questions: which receptors were involved in PGD₂ modulation of bladder detrusor contractility and what was the location of the receptors involved. We also wished to explore the site of formation of

PGD₂ by studying the distribution of PGD synthase (PGDS). The present study showed that, in the guinea pig, urinary bladder, PGDS was very abundant in the suburothelium and that PGD₂ inhibited the contractile responses to electrical field stimulation (EFS), and to ACh and ATP, probably via DP₁ receptors localized in the smooth muscle. PGD₂ at high concentration also activated TP receptors, enhancing the contractile responses to EFS.

Methods

Animals

All animal care and experimental procedures complied with the EEC/EU guidelines (Directive 86/609/EEC and Directive 2010/63/EU) on the protection of animals used for scientific purposes and were approved by the Stockholm North animal ethics committee (Dnr N148/08, N178/11). All efforts were made to minimize animal suffering. Experimental procedures involving animals are reported in accordance with the ARRIVE guidelines (Kilkenny *et al.*, 2010; McGrath *et al.*, 2010).

We used 37 albino Dunkin Hartley guinea pigs (strain HsdDhl:DH; Harlan Laboratories, Boxmeer, The Netherlands) of either sex weighing 350–550 g which were maintained on a 12:12 h light/dark cycle at 20 ± 1°C and had free access to food [Labfor K1 Special, Lantmännen Kimstad, Sweden, complemented with Timothy Cubes (#F1011), Datesand Ltd, Manchester, UK] and water in an enriched environment.

Tissue preparation for organ bath experiments

Experiments were commenced in the morning. The animals were anaesthetized with midazolam (1 mg·kg⁻¹) and sodium pentobarbital (120 mg·kg⁻¹) i.p. and exsanguinated. The abdomen was opened by a midline incision. The urinary bladder was separated from the urethra and ureters and cleaned from fat and connective tissue. The trigone of the urinary bladder was removed by identifying the location of urethra and ureter openings. Detrusor strips (8 × 2 mm) were then cut from the remaining bladder dome. The urothelium was removed as much as possible by fine dissection with scissors under the microscope, a procedure which also removes the suburothelium (Munoz *et al.*, 2010; Birder *et al.*,

2012). The urothelium-free detrusor strips were then tied at both ends with thin cotton threads and were equilibrated in a storage bath for at least 60 min in modified Tyrode's solution (136.9 mM NaCl, 4.8 mM KCl, 23.8 mM NaHCO₃, 0.5 mM MgCl₂, 0.4 mM NaH₂PO₄, 2.5 mM CaCl₂ and 5.5 mM glucose) and aerated with 5% CO₂/95% O₂.

After equilibration, urothelium-denuded bladder strips were transferred to 2.5–6.5 mL organ baths with aerated Tyrode's solution. One end of the tissue was connected to an isometric transducer and the other end to a hook at the bottom of the bath and the resting tension of the bladder strips was adjusted to 10 mN. Tissues were washed three times and tension was readjusted to 10 mN and then not further adjusted. When subsequently the resting tension was stable for at least 15 min, preparations were electrically stimulated by means of two platinum electrodes on the walls of the organ baths (50 V, single pulses of 0.2 ms every 30 s). The evoked contractions were recorded with a computerized acquisition system (MP100; Biopac Systems, Inc., Goleta, CA, USA). After stabilization, diclofenac (10⁻⁶ M) was added to the bath. After 10 min incubation with diclofenac, the tissues were then washed and diclofenac (10⁻⁶ M) was reapplied to the bladder strips and remained throughout the experiment. After at least another 30 min, agonists were applied to the tissue cumulatively in half-log increments both in the presence and absence of antagonists. Tissue strips were exposed to antagonists for at least 1 h due to the high lipophilicity and slow onset of PG receptor antagonists.

Organ bath experimental procedures

PGD₂ effects on guinea pig detrusor contractions induced by nerve stimulation. PGD₂ was applied cumulatively to the tissues in half-log increments from 10⁻⁹ to 10⁻⁶ M. The tissue was exposed for 8–10 min to each dose until a stable effect was developed. The contractile response amplitude to EFS was also measured before application of PGD₂. This value was set to be 100% (control amplitude). Log concentration–response curves were constructed with the percentage comparison between contractile amplitude at each concentration of PGD₂ and the control amplitude.

PGD₂ effects on contractions in the presence of DP₁ and/or TP receptor antagonists. The DP₁ receptor antagonist BW-A868C (10⁻¹⁰, 10⁻⁸ and 10⁻⁶ M) and the TP receptor antagonist SQ-29548 (10⁻⁷ M) were separately applied to tissues. After 1 h incubation with antagonists, PGD₂ was applied to the tissues cumulatively in half-log increments from 10⁻⁹ to 10⁻⁶ M. In another group of experiments, the effect of BW-A868C (10⁻⁶ M) and SQ-29548 (10⁻⁷ M) in combination was investigated. Similar PGD₂ dose–response curves from 10⁻⁹ to 10⁻⁶ M were then performed on the detrusor strips. The contractile response amplitude (control amplitude) was measured 1 h after antagonist application but before PGD₂ administration, and set as 100%. As studies had shown that BW-A868C as a DP₁ receptor antagonist had partial agonist effect in, for example, dog tracheal epithelium (Liu *et al.*, 1996), this was also studied and compared with the DP₁ receptor agonist BW-245C. To analyse the antagonist effects of BW-A868C on the guinea pig detrusor, dose–response curves were generated by the DP₁ receptor agonist BW-245C

from 10⁻¹⁰ to 10⁻⁶ M cumulatively in log increments also in the presence of BW-A868C (10⁻⁸ and 10⁻⁷ M).

Solvent effects on guinea pig detrusor contractions. All the solvents used in dissolving the agonist and antagonist were tested under the same condition on guinea pig detrusor strips. The same amount of solvent used in dissolving agonist was given cumulatively to the tissue. The final concentration of solvent used in each organ bath was less than 0.1% ethanol.

Western blot analysis

Guinea pigs were anaesthetized as above, the abdomen was opened and the descending aorta was perfused with 30–40 mL warm saline to achieve blood-free tissues after which the bladder dome was isolated as described above. Separate tissue samples of either intact wall, urothelium with suburothelium, or muscle were prepared. For protein extraction, each mg wet tissue was subjected to 20 µL of lysis buffer (pH 7.6) containing 20 mM HEPES, 150 mM NaCl, 5 mM EDTA, 25 mM KF, 1 mM sodium orthovanadate, 0.5% Triton X-100, 20% glycerol and 1% protease inhibitor cocktail (Sigma-Aldrich, St. Louis, MO, USA). Tissue was homogenized using an Ultra-Turrax for 2 min and then transferred to a Dounce homogenizer with continued homogenization for 4 min. Lysates were centrifuged at 13 000× *g* for 20 min at 4°C. Protein content of the supernatant was determined with the Bradford protein assay (Bio-Rad Laboratories, Inc., Hercules, CA, USA). Up to 50 µg of protein was loaded onto 8–16% SDS Pierce ProteinGel (Thermo Scientific Inc., Waltham, MA, USA) and separated by electrophoresis. Proteins were transferred onto PVDF membranes using dry blot/iBLOT according to the manufacturer's instructions (Invitrogen brand, Thermo Scientific). Membranes were blocked for 1 h with 5% skim milk dissolved in PBS-T (PBS, 0.1% Tween 20). Membranes were probed for 1 h at room temperature with a full-length rabbit anti-human haematopoietic PGDS antibody (1:200; sc-30066, Santa Cruz Biotechnology Inc, Dallas, TX, USA), a rabbit anti-human DP₁ receptor antibody (1:1000; ab99446, Abcam, Cambridge, UK) or a mouse IgG1 anti-human β-actin antibody (1:40 000; Sigma-Aldrich, A5441) diluted in PBS-Tween 20 with 5% skim milk. HRP-conjugated goat anti-rabbit (1:6000; Thermo Scientific) or goat anti-mouse secondary antibodies (1:10 000; Thermo Scientific) and Supersignal West Femto Chemiluminescent Substrate (Thermo Scientific) were used to detect protein signal on autoradiographs (Kodak X-Omat 2000 processor; Kodak, New York, NY, USA).

Immunofluorescence and microscopy

Guinea pigs were anaesthetized and perfused as above. The urinary bladder was isolated and cleaned from connective tissues and then fixed by immersion in ice-cold 4% paraformaldehyde 0.1 M phosphate buffer fixative solution for 4 h at 4°C. After fixation, tissues were cryoprotected by incubation in 0.1 M phosphate buffer with 30% sucrose solution for 16–20 h at 4°C. Bladder tissues were covered with Neg-50 (Thermo Scientific) and quickly frozen in liquid nitrogen-cooled isopentane and stored at –80°C. Transverse bladder dome sections were cut at 10 µm thickness using an HM 525 cryostat (MICROM International GmbH, Walldorf, Germany). Sections were mounted on gelatin-coated slides.

Immunofluorescence. Cryostat sections were blocked in blocking buffer PBS (pH 7.2) containing 0.5% Triton X-100 and 5% normal goat serum for 20 min at room temperature. Sections were labelled with a rabbit anti-human haematopoietic PGDS antibody (1:100; Santa Cruz, sc-30066), a rabbit polyclonal antibody raised against human DP₁ receptor C-terminal (1:250; Abcam, ab99446) or a rabbit anti-human DP₂ (CRTH2) receptor antibody (1:2000; NBP1-76755, Novus Biologicals LLC, Littleton, CO, USA) diluted in blocking buffer overnight at 4°C. To visualize the basal membrane and neuronal cell bodies and processes, sections were incubated for 1 h at room temperature with a rabbit anti-laminin antibody (1:200; Sigma-Aldrich, L9393) or a chicken anti-human PGP 9.5 (protein gene product 9.5) antibody (1:500; Abcam, ab72910) diluted in blocking buffer. The sequential control sections were treated with blocking buffer without primary antibody. Sections were washed three times for 5 min in PBS followed by application of secondary donkey anti-rabbit antibody labelled with Alexa Fluor 568 (1:500; Invitrogen, A10042), donkey anti-rabbit antibody labelled with Alexa Fluor 488 (1:500; Invitrogen, A-11055) or goat anti-chicken IgY H&L labelled with Alexa Fluor 488 (1:500; Abcam, ab150173) for 1 h at room temperature. Fluorescein isothiocyanate-labelled phalloidin (1:1000; Sigma-Aldrich, P5282) or a mouse Cy3-conjugated anti- α -smooth muscle actin antibody (Sigma, C6198) for actin visualization was applied together with secondary antibody and nuclei were counterstained with Hoechst 33258 (1:2000; Sigma-Aldrich, 94403). After 1 h incubation, sections were washed for 5 min three times in PBS in the dark. The sections were then mounted with mounting medium with anti-fading agent (S3023; Dako Sweden AB, Stockholm, Sweden) and covered with coverslips.

Microscopy. All immunolabelled sections were observed under an Axioplan 2 imaging fluorescence microscope (Carl Zeiss MicroImaging GmbH, Jena, Germany) equipped with FITC (Chroma 41001), TRITC (Chroma 41002a) and DAPI (Chroma #31000) filters. Sections were photographed with a Nikon D300 digital camera (Nikon Corporation, Chiyoda, Tokyo, Japan). The software NKRemote version 2.2 (Breeze Systems, Camberley, Surrey, UK) was used for camera control with 12 bit image acquisition followed by subsequent background subtraction and contrast enhancement in ImageJ (NIH open source).

Data analysis

Agonist and antagonist characteristics were analysed using Prism 5 (GraphPad Software Inc., La Jolla, CA, USA). Western blots were quantitatively evaluated by the gels, plot lanes and routine in ImageJ, and the relative amount of protein in a tissue component was expressed in per cent of the sum of that protein in all tissue components. All data are presented as mean \pm SEM. Student's unpaired two-sided *t*-test and one-way ANOVA were used for comparison of IC₅₀ values and differences between several groups.

Materials

PGD₂ was a generous gift from Professor Ernst H Oliw (Uppsala Universitet, Uppsala, Sweden). SQ-29548 was from Cayman Chemical (Ann Arbor, MI, USA). BW-245C and

BW-A868C were from Synchem UG & Co. KG (Felsberg/Altenburg, Germany). Stock solutions (10⁻³ M) of PGD₂, BW-245C, SQ-29548 and BW-A868C were made in ethanol. Further dilutions of compounds were prepared with distilled water before experiments. Diclofenac, propranolol and routine chemicals were purchased from Sigma-Aldrich.

Results

PGD₂ and DP₁ receptor agonist mediated inhibition of detrusor contractile responses induced by nerve stimulation

In the guinea pig urinary bladder, PGD₂ was previously shown to inhibit the EFS-induced contractions both in the urothelium-intact and the urothelium-denuded strips with significantly different efficacies (Guan *et al.*, 2014). Thus, the effects of prostanoids and specifically PGD₂ are much more prominent in urothelium-denuded and diclofenac-treated tissues, probably due to a high urothelium-dependent PG release in urothelium-intact tissue (Guan *et al.*, 2014). In order to minimize any interfering effect by endogenous prostanoids in our pharmacological analysis, the effects of PGD₂ on contractile responses evoked by EFS or by agonists were studied, here, in urothelium-denuded guinea pig bladder strips in the presence of diclofenac. We previously found the current mode of stimulation to elicit contractions that are mediated by a simultaneous ATP- and ACh-mediated neuroeffector transmission (Guan *et al.*, 2014). As expected, these responses were inhibited by PGD₂ in a dose-dependent manner (Figure 1, top panel). The estimated pIC₅₀ was 7.55 \pm 0.15 (*n* = 13) (Figure 2). A dominant postjunctional inhibitory effect may be suggested as contractile responses to exogenous ATP were also inhibited by PGD₂ (Supporting Information Fig. S1), in agreement with previous observations (Guan *et al.*, 2014). The inhibitory action of PGD₂ on EFS-induced contractile responses was not modified by the β -adrenoceptor antagonist propranolol (Supporting Information Fig. S2). Even at 10⁻⁶ M PGD₂ did not fully inhibit the contractile responses to EFS (Figure 2). The inhibitory effects by PGD₂ on contractile responses to EFS were mimicked by the DP₁ receptor agonist BW-245C. BW-245C was a full agonist and was more potent than PGD₂ with a pIC₅₀ of 8.11 \pm 0.07 (*P* < 0.02, *n* = 11) (Figure 3).

Antagonism of DP₁ receptor-mediated inhibition and TP receptor-mediated excitation

The DP₁ receptor antagonist BW-A868C (10⁻⁸ to 10⁻⁶ M), in addition to a slight agonist effect of its own (Figure 3), caused a progressive dose-dependent reversal of the PGD₂ inhibitory effect on the contractile responses to EFS, where first the higher concentrations of PGD₂ (during BW-868C 10⁻⁸ M) and then all concentrations of PGD₂ (during BW-868C 10⁻⁶ M) now evoked an enhancing effect on the contractile responses (Figure 1, two middle panels). In the presence of BW-868C (10⁻⁶ M), the pEC₅₀ for the PGD₂-enhancing effect was 6.51 \pm 0.30 (*n* = 8), which is significantly lower than for the inhibitory effect of PGD₂ in the absence of antagonists (*P* < 0.01). The enhancement by PGD₂, after blocking DP₁ receptors with BW-A868C, was antagonized by the TP receptor antagonist

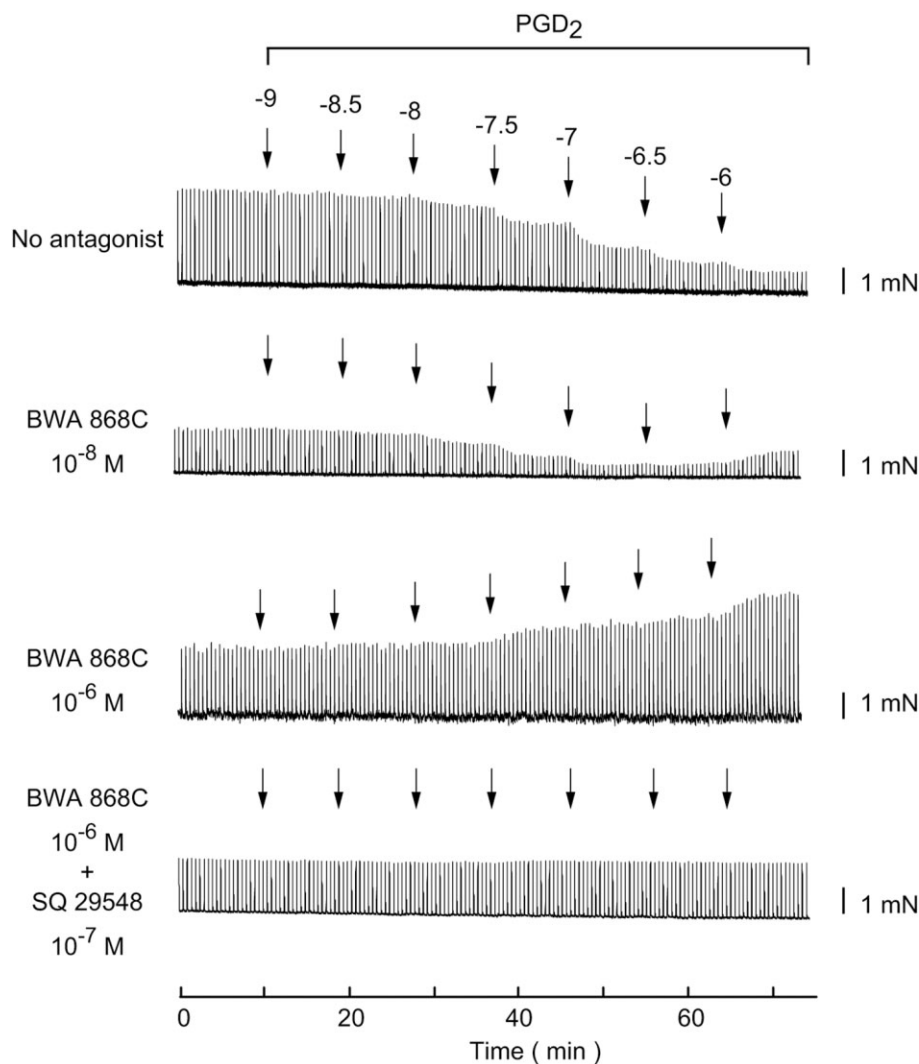


Figure 1

Experimental recordings showing PGD_2 effects at indicated log M concentrations on isometric contractile responses in guinea pig urothelium-denuded diclofenac-treated detrusor strips evoked by EFS (50 V, single pulses of 0.2 ms every 30 s). Upper panel illustrates the effect of addition of increasing concentrations of PGD_2 under control conditions. Middle two panels show the effects of PGD_2 in the presence of a moderate (10^{-8} M) and a relatively high (10^{-6} M) concentration of the DP_1 receptor antagonist BW-A868C, respectively, where the higher concentration abolishes the inhibitory effect of PGD_2 and changes it into an enhancing effect. Lower panel shows that the enhancing effect by PGD_2 in the presence of the DP_1 receptor antagonist BW-A868C (10^{-6} M) is abolished by the TP receptor antagonist SQ-29548 (10^{-7} M). Time between PGD_2 applications (arrows) was 8–10 min.

SQ-29548 (10^{-7} M; Figure 1 lower panel and Figure 2). SQ-29548 (10^{-7} M) alone (i.e. in the absence of BW-A868C) did not modify the effect of PGD_2 (Figure 2).

BW-A868C is known to be a partial agonist at DP_1 receptors. The agonist profile of BW-A868C in the guinea pig urinary bladder strips was therefore investigated. Compared with the DP_1 receptor agonist BW-245C dose–response curve, the BW-A868C dose–response curve was shifted up and to the right (Figure 3A). Estimating the potency of BW-A868C as agonist yielded a pIC_{50} of 7.68 ± 0.28 ($n = 9$). The pharmacological characteristic of BW-A868C as antagonist in guinea pig urinary bladder was investigated by performing cumulative BW-245C dose–response curves in the absence and

presence of BW-A868C at different concentrations (Figure 3B). The agonist dose–response curves were shifted to the right by BW-A868C, yielding an apparent pA_2 of 8.68 ± 0.06 ($n = 6$) (Figure 3B).

Solvent effects on guinea pig detrusor strip contractions induced by EFS

In vehicle controls, solvent alone within the volume limit of 0.1% ethanol final bath concentration and administered to tissues, at the same duration as in drug experiments, did not modify tone or contractile responses to EFS in the guinea pig bladder strips.

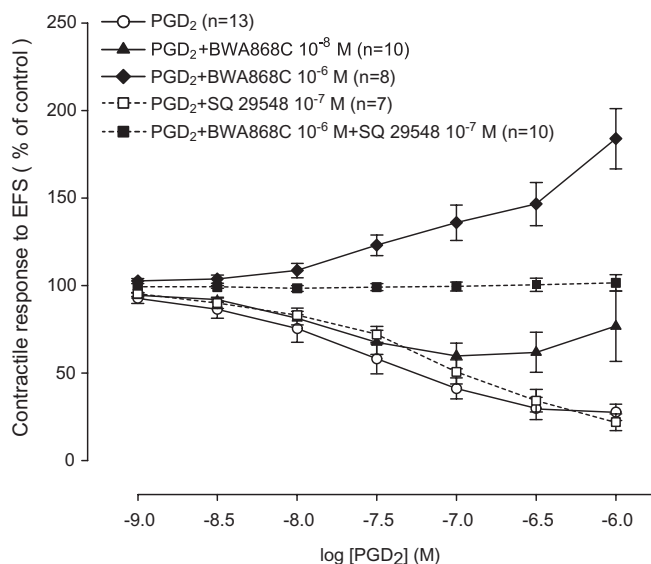


Figure 2

Cumulative dose-response curves to PGD₂, in the absence and presence of DP₁ receptor antagonist BW-A868C and/or TP receptor antagonist SQ-29548, on contractile responses in urothelium-denuded diclofenac-treated guinea pig urinary bladder detrusor strips evoked by EFS (50 V, single pulses of 0.2 ms every 30 s). Data presented as mean \pm SEM, *n* denotes the number of tissues, and the number of animals used for each curve was from 4 to 8. Data for 8 of the 13 control tissues are from Guan *et al.* (2014).

Expression of haematopoietic PGDS and DP₁ receptors in the guinea pig bladder

The expression of haematopoietic PGDS and DP₁ receptor protein in the guinea pig bladder was examined by Western blot. The whole bladder dome extract, as well as the dome detrusor muscle and dome urothelium extracts, was exposed to anti-PGDS and anti-DP₁ receptor antibodies, which were the same antibodies used in the immunofluorescence histochemistry. As shown in Figure 4A, a band between 24 and 31 kD indicating haematopoietic PGDS protein was found to be present in guinea pig urinary bladder dome at a position predicted from the information supplied by the manufacturer. The bar graph in Figure 4A shows significant differences in PGDS protein expression between the urothelium tissue and the detrusor muscle tissue which agrees with a strong urothelium dependency in the release of PGD₂ from the guinea pig urinary bladder (Guan *et al.*, 2014). In the extract analysed in the Western blot, our method for isolating the urothelium leads to inclusion of the suburothelium (Munoz *et al.*, 2010; Birder *et al.*, 2012) which should be noted when interpreting the immunohistochemistry data in the following section.

The guinea pig urinary bladder dome expressed significant amounts of DP₁ receptor protein (Figure 4B). A protein band between 40 and 50 kD was seen with the predicted size for DP₁ receptor protein. This result fits the data provided by the manufacturer who tested the antibody on different cell lines. The summary of DP₁ receptor protein expression in the different tissue components indicated significantly less DP₁ receptor protein expressed in the urothelium compared with that in the detrusor muscle (Figure 4B bar graph).

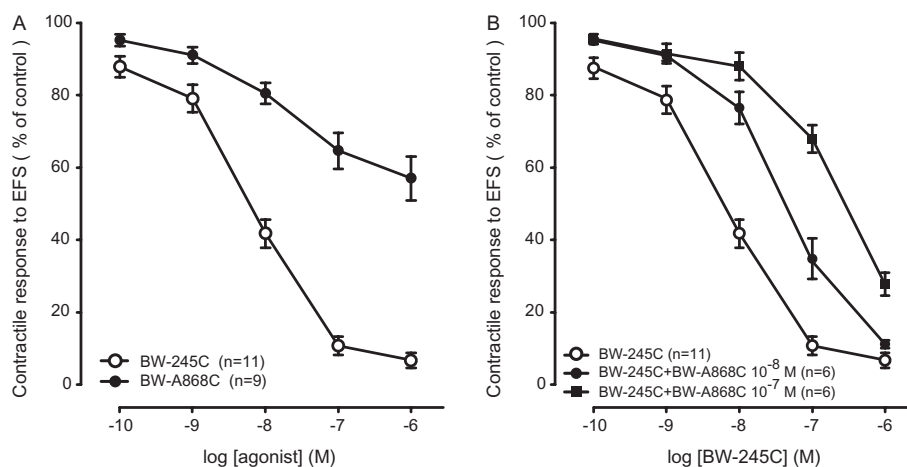


Figure 3

Agonism and antagonism by PGD₂ analogues on contractile responses in urothelium-denuded diclofenac-treated guinea pig urinary bladder detrusor strips evoked by EFS (50 V, single pulses of 0.2 ms every 30 s). Panel A: cumulative dose-response curves to the selective DP₁ receptor agonist BW-245C and the partial DP₁ receptor agonist BW-A868C. Panel B: cumulative dose-response curves to the DP₁ receptor agonist BW-245C in the absence and presence of the DP₁ receptor antagonist BW-A868C. Panel A shows that BW-A868C has agonist activity and therefore this effect has been compensated for in panel B which shows that BW-A868C causes a rightward shift of the dose-response curve of the agonist BW-245C. Data presented as mean \pm SEM, *n* denotes the number of tissues, and the number of animals used for each curve was from 3 to 4.

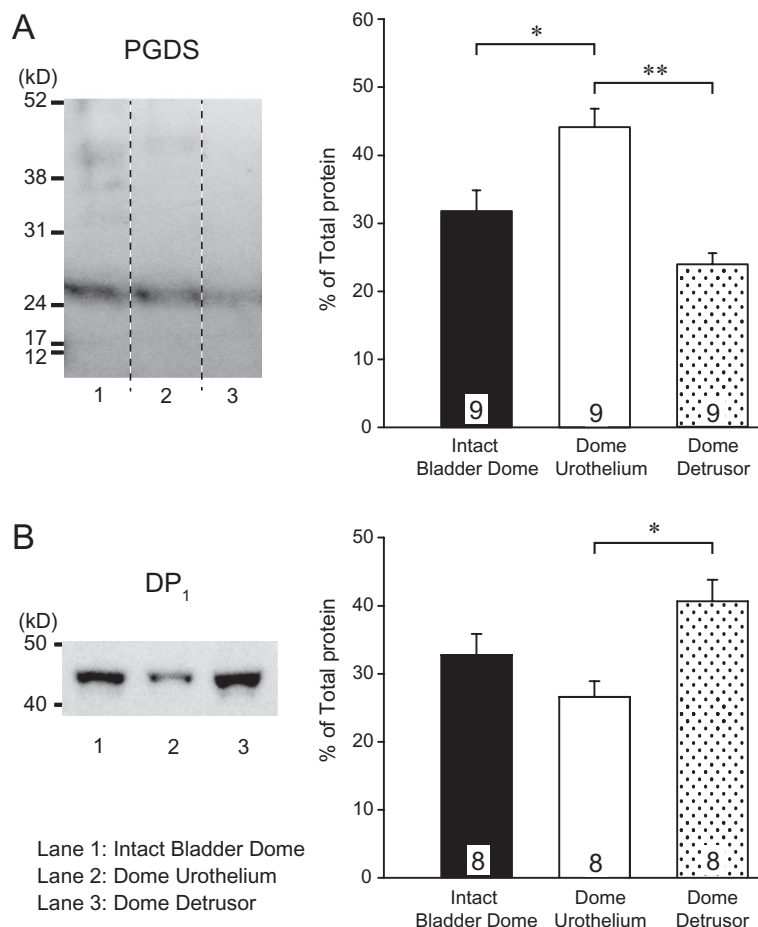


Figure 4

Western blots and summaries of protein expression in whole guinea pig urinary bladder wall (intact bladder dome) and separated urothelium (dome urothelium) and detrusor muscle tissues (dome detrusor) respectively. (A) Haematopoietic PGDS protein and (B) DP₁ receptor protein. Data were acquired from eight or nine lanes (indicated within each bar) for each group and presented as mean \pm SEM. Tissue extracts were from four to six animals, * $P < 0.05$, ** $P < 0.01$; significantly different as indicated; one-way ANOVA.

Distribution of haematopoietic PGDS and DP₁ receptor in the guinea pig bladder

Smooth muscle and nuclei were labelled separately by smooth muscle actin antibody in red and Hoechst 33258 nuclear stain in blue as shown in Figure 5C and E. The smooth muscle was relatively faintly labelled with anti-PGDS antibody compared with urothelium/suburothelium (Figure 5D). No staining was obtained in the secondary antibody control (Figure 5B) which was a sequential section of that in Figure 5A. Staining for actin was prominent in the detrusor muscle and also in vessels of the lamina propria (Figure 5C), with only minor overlap with the PGDS stain (Figure 5D). In order to identify the urothelium, basal membrane staining was performed with anti-laminin in combination with nuclear stain (Figure 6). In Figure 6C, it can be seen that a basal row of cell nuclei lines up in the urothelium just above the basal membrane laminin stain. In comparison, the similar lining up of nuclei allows the major PGDS stain to be determined as localized to the suburothelium (Figure 5F).

Immunoreactive DP₁ receptors were seen in several cell types throughout the guinea pig urinary bladder, as visualized

by the red stain in Figure 7A. The urothelium basal membrane was identified by the nuclear stain profile as determined in Figure 6 and is indicated by dashed lines in Figure 7A and B, suggesting that there was only minor to moderate staining for DP₁ receptors in the urothelium and a more pronounced staining in the suburothelium. The most prominent staining for DP₁ receptors was in the detrusor muscle (Figure 7A and B) and in vessel smooth muscle (Figure 7C and D). However, at higher magnification, it was evident that urothelial cells also stained for DP₁ receptors, and that interstitial cell-like profiles in the suburothelium, and especially their cell membranes, stained for DP₁ receptors (Figure 7E) as supported by vimentin staining (Supporting Information Fig. S3). Very few such profiles could be seen stained for DP₁ receptors within the muscle cell layer. In the urothelial cells (Figure 7E) and especially in the smooth muscle (Figure 7F), the DP₁ receptor localization was mainly in the cell membrane, although intracellular staining could also be seen. Mast cells were neither observed in the guinea pig urinary bladder cryostat sections stained for PGDS nor when stained for DP₁ receptors.

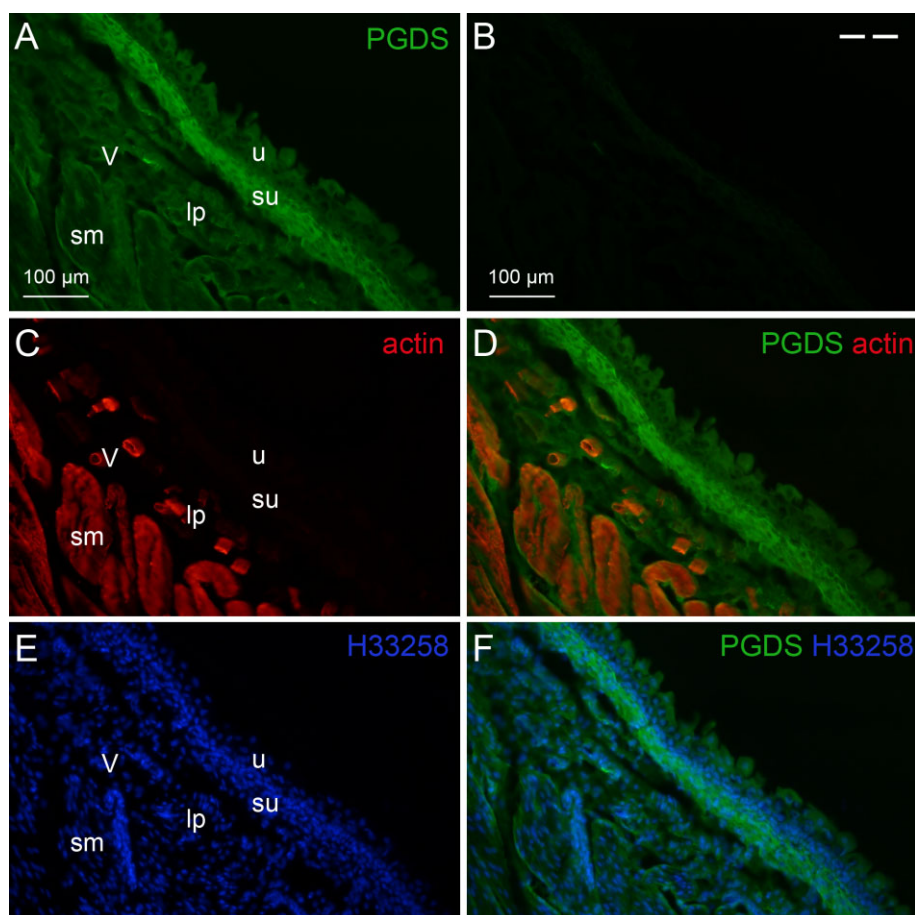


Figure 5

Distribution of haematopoietic PGDS in the urothelium and smooth muscle of guinea pig urinary bladder. Fluorescence immunohistochemistry of transverse section of male guinea pig bladder dome (A–F) as indicated. Panel A: immunofluorescence with PGDS antibody (green). Panel B: adjacent section to panel A incubated with secondary antibody only. Panel C: section in panel A showing immunofluorescence staining with anti- α -smooth muscle actin antibody (red). Panel D: superposition of images A and C. Panel E: nuclear staining with Hoechst 33258 (H33258; blue) in section of panel A. Panel F: superposition of images in panels A and E. Symbols legend: u denotes urothelium, lp denotes the deep part of lamina propria, su denotes the immediate suburothelium of lamina propria, sm denotes smooth muscle, V denotes blood vessels in the lamina propria.

Double labelling of DP₁/DP₂ receptors and PGP 9.5 in the guinea pig bladder

Immunoreactivity to DP₁ and DP₂ receptors was distributed differently among different tissues. Unlike DP₁ receptors predominantly distributed in the smooth muscle cells (Figure 7 and Figure 8E), DP₂ receptors were mainly distributed in the urothelium (Supporting Information Fig. S4). DP₁ and DP₂ receptors were both seen distributed in the suburothelium layer with different staining profiles (Figure 8A and Supporting Information Fig. S4). The distribution of nerve profiles was visualized by using anti-PGP 9.5 antibody and only a few profiles were seen in the suburothelium whereas several were seen in the smooth muscle layer (Figure 8B and F, and Supporting Information Fig. S4B and F). Double labelling of DP₁ receptors and PGP 9.5 indicated no co-localization in the urothelium and smooth muscle (Figure 8C and G) but, in the suburothelium layer, the cell membranes of PGP 9.5-positive interstitial cell-like profiles showed positive staining for DP₁

receptors (Figure 8C). Double labelling of DP₂ receptors and PGP 9.5 showed co-localization in the urothelium, but not in the suburothelium and smooth muscle (Supporting Information Fig. S4C and G).

Discussion and conclusion

The present study shows that the neuroeffector transmission in guinea pig urinary bladder can be modulated by a combined DP₁ receptor-mediated inhibitory and a TP receptor-mediated enhancing action. According to the BPS/IUPHAR prostanoid receptors classification, there are nine prostanoid receptors and those preferentially activated by PGD₂ are classified as DP₁ and DP₂ (CRTH2) although activation of other receptors, notably TP receptors, has also been reported (Woodward *et al.*, 2011). These receptors are typical 7-transmembrane GPCR, and G-protein coupling studies clas-

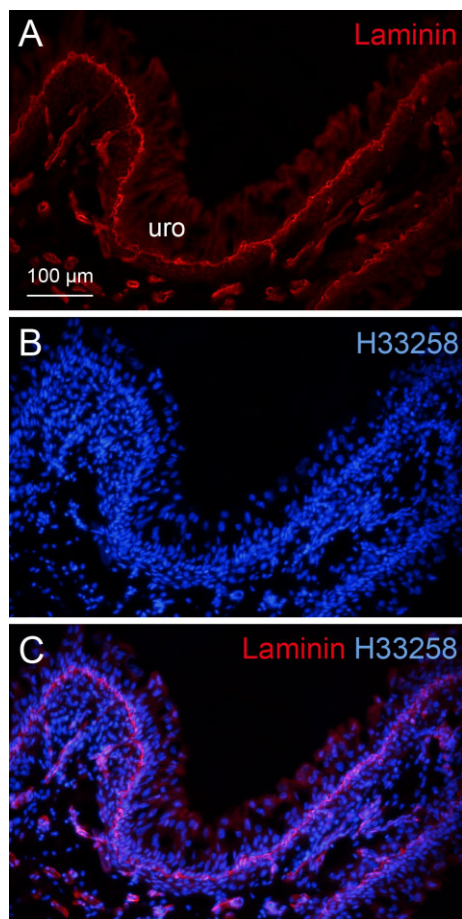


Figure 6

Fluorescence immunohistochemistry of transverse section of the guinea pig bladder dome showing the location of urothelium basal membrane. Panel A: staining with antibody against laminin (red). Panel B: staining with the nuclear stain H33258 (blue). Panel C: superposition of images in panels A and B. The label uro denotes the faintly stained urothelial epithelial cells above the laminin-stained basal membrane.

sified DP₁ receptors as G_s-coupled receptors, DP₂ as G_i-coupled receptors, and TP receptors as G_q-coupled receptors. In smooth muscle, activation of G_s-coupled receptors leads to increase of the intracellular cAMP level, in turn activating PKA which through phosphorylation of myosin light chain kinase results in smooth muscle relaxation. This fits our result that DP₁ receptors had an inhibitory influence on guinea pig urinary bladder contractility, and the presently observed dominant localization of DP₁ receptors to the smooth muscle membranes also fits this model. TP receptors can increase the intracellular Ca²⁺ level. The present enhancing effect by PGD₂ on contractile responses generated after blockade of DP₁ receptors was through activation of TP receptors as evidenced by the blocking effect of the TP receptor antagonist SQ-29548, and a likely explanation might be an action through increased intracellular Ca²⁺, although other mechanisms cannot be excluded (Fernandes *et al.*, 2013). The

present dose–response data for the enhancing effect by PGD₂, in the presence of the DP₁ receptor antagonist BW-A868C, suggest that the TP receptor-mediated effect by PGD₂ is exerted at slightly lower potency, although the data have to be interpreted with caution due to the partial agonist effect by BW-A868C. An effect by PGD₂ through TP receptors is in agreement with ligand binding studies using CHO cells expressing mouse prostanoid receptors, showing that PGD₂ binds not only to DP₁, but at low potency to TP receptors (Kiriya *et al.*, 1997). PGD₂ exerted inhibitory effects on contractile responses to nerve stimulation, on responses to the neurotransmitters ACh and ATP (Guan *et al.*, 2014), and the inhibition of EFS-induced contractions was not modified by non-selective β -adrenoceptor blockade. It can therefore be concluded that PGD₂ mainly acts via a postjunctional inhibitory effect exerted via DP₁ receptors. From the present results, however, additional prejunctional effects by PGD₂ cannot be excluded.

The present data show that PGDS expression was found in the urothelium and the immunohistochemistry revealed this to be reflected by immunoreactivity in the urothelium and especially in the suburothelium. This agrees well with our previous data showing a strong urothelium dependence in the release of PGD₂-like bioactivity from the bladder (Guan *et al.*, 2014) and with our data shown here, when we have used a method for urothelium removal which also removes the suburothelium (Munoz *et al.*, 2010; Birder *et al.*, 2012). In the urothelium-intact, non-diclofenac-pretreated, bladder tissues, high endogenous PG concentrations obscured the effects of additional application of exogenous PGs (Guan *et al.*, 2014). Therefore, we currently used urothelium-denuded, diclofenac-pretreated, bladder tissues to investigate the exogenous PGD₂ modulation and receptors involved in guinea pig bladder regulation. Whether PGD₂ may modulate human bladder motility and a disturbed PGD₂ function might have a role in overactive bladder syndrome (OAB) merits further investigation, taking into consideration the possibility of a high endogenous PGD₂ formation.

A previous study reported on the localization of COX-1 immunoreactivity in the guinea pig urinary bladder (de Jongh *et al.*, 2009). In this study, the strongest localization of COX was in the urothelium as compared with the suburothelium, and only a subset of suburothelial cells exhibited staining for COX-1. In the rabbit, the suburothelial interstitial cells also expressed COX-2 (Collins *et al.*, 2009). Thus, it is possible that the substrate for PGDS might be provided by both types of COX. Considering our observation that PGDS was widely distributed in the suburothelial cells, and the observation by de Jongh *et al.* that the basal urothelial cells are especially rich in COX, leads to the possibility that a transcellular metabolism is involved such that the basal urothelial cells donate the precursor PGH₂ for further metabolism by the suburothelial PGDS to PGD₂. Transcellular metabolism is well known for arachidonate transformation by lipoxygenase pathways (Marcus *et al.*, 1987; Gronert *et al.*, 1999) and has previously been shown for the synthesis of PGE₂ from precursor donated by vascular endothelial cells to tumour cells (Salvado *et al.*, 2009). Such a mechanism in urothelium–suburothelium interaction merits further analysis in future studies, and if proven would add to the concepts

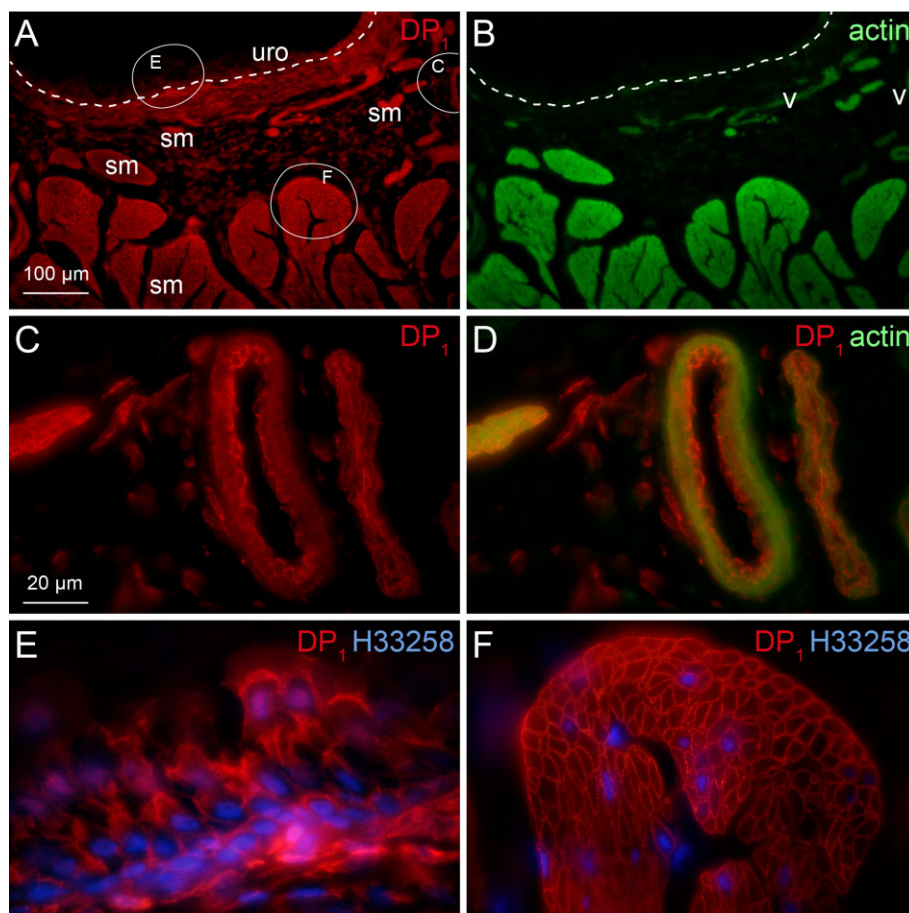


Figure 7

Distribution of DP₁ receptors in the guinea pig urinary bladder wall. Fluorescence immunohistochemistry of transverse section of male guinea pig bladder dome (A–F) as indicated. Panel A: immunofluorescence with DP₁ receptor antibody (red). Panel B: section in panel A showing staining with phalloidin actin stain (green). Panel C: region denoted C in panel A at higher magnification showing immunofluorescence staining of DP₁ receptors in vessel wall (red). Panel D: superposition of staining for DP₁ receptors (red) and actin (green) at higher magnification of region C from panel A. Panel E: combined immunofluorescence for DP₁ receptors (red) and nuclear stain with H33258 (blue) at higher magnification of region E from panel A showing staining for DP₁ receptors in urothelium and intense staining in some elongated cell profiles in the immediate suburothelium, most likely representing interstitial cell-like profiles. Panel F: combined immunofluorescence for DP₁ receptors (red) and nuclear stain with H33258 (blue) at higher magnification of region F in a transversely cut bundle of the bladder wall smooth muscle at F from panel A showing intense staining for DP₁ receptors in the smooth muscle cell membranes. Symbols legend: dashed lines in A and B denote position of urothelium basal membrane, sm denotes smooth muscle, uro denotes urothelium, v denotes vessels.

of signalling between the urothelium, interstitial cells and muscle (Fry *et al.*, 2007; Birder *et al.*, 2012; Birder and Andersson, 2013).

In the present series of experiments, strong immunoreactivity for DP₁ receptors was found in the smooth muscle, with a marked localization to the cell membranes. This agrees with the inhibitory effect by PGD₂ on contractile responses to EFS and on responses to exogenous agonists (Guan *et al.*, 2014). It is also in agreement with the blockade by the DP₁ receptor antagonist BW-A868C. Several roles of PGs in regulating not only smooth muscle contractility but also other cellular functions such as interstitial cells and afferent nerves have been considered (Collins *et al.*, 2009; de Jongh *et al.*, 2009; Rahnama'i *et al.*, 2012). Several populations of interstitial cell-like profiles are found throughout the guinea pig bladder wall, and are making contact with neurons (Davidson and

McCloskey, 2005). In guinea pig bladder base suburothelium and bladder urethral junction lamina propria, a group of vimentin-positive interstitial cell-like profiles is also positively stained for PGP 9.5 (Grol *et al.*, 2008). The present observations showing strong DP₁ receptor immunoreactivity on membranes of vimentin- and PGP 9.5-positive interstitial cell-like profiles in the suburothelium (Figure 8, Supporting Information Fig. S3) and in the urothelial cell membranes suggest that PGD₂ might be involved also in other pathways such as in sensing functions in these cell types.

Some limitations of this study need to be addressed. This was an *in vitro* experiment designed by using guinea pig urothelium-denuded urinary bladder strips. Studies *in vivo* would provide us important information about the effect of PGD₂ and receptor antagonists in the whole urinary system in the presence of an intact urothelium. In our previous study

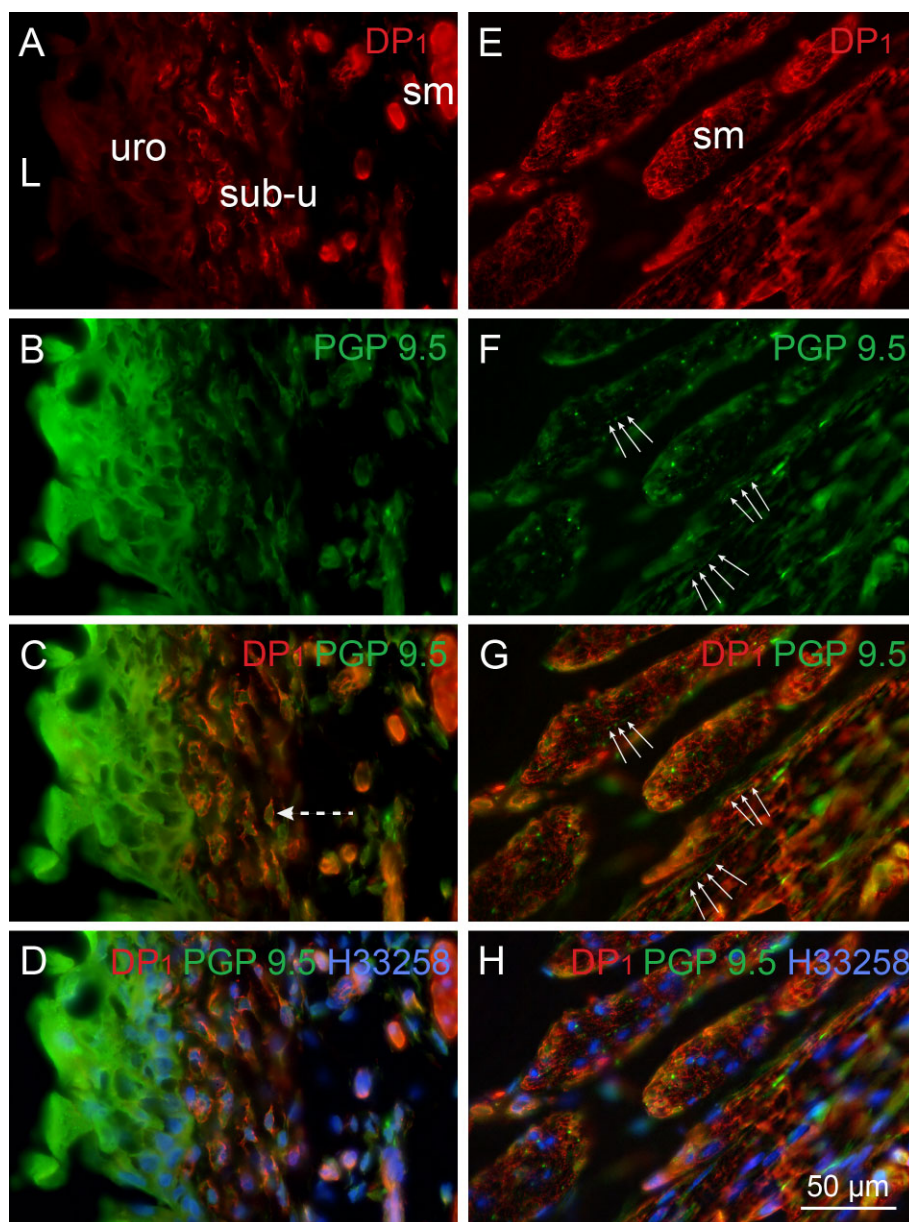


Figure 8

Distribution of DP₁ receptors in the guinea pig urinary bladder wall and comparison with the distribution of the neuronal marker protein PGP 9.5. Fluorescence immunohistochemistry of transverse section of male guinea pig bladder dome (A–H) as indicated. Panels A and E: immunofluorescence with DP₁ antibody (red). Panels B and F: same section, stained with antibody against PGP 9.5 (green). Panels C and G: superposition of staining for DP₁ receptors (red) and PGP 9.5 (green). Panels D and H: combined immunofluorescence for DP₁ receptors (red), PGP 9.5 (green) and nuclear stain with H33258 (blue). Arrows in panels F and G indicate nerve-like profiles stained for PGP 9.5, dashed arrow in panel C denotes one of several interstitial cell-like profiles, uro denotes urothelium, sub-u denotes suburothelium, sm denotes smooth muscle.

(Guan *et al.*, 2014), we concluded that PGD₂ and PGE₂ were released *in vitro* from guinea pig urinary bladder, suggesting that endogenous PGD₂ and PGE₂ might be continuously modulating the contractility in guinea pig urinary bladder. The dominant effect *in vitro* must be an enhancing effect by PGE₂ as responses are inhibited by COX inhibition (Guan *et al.*, 2014). Whether a concomitant inhibitory influence by PGD₂ is also at hand cannot be deduced as the DP₁ antagonist

presently used is also a partial agonist, precluding its use to antagonize endogenous PGD₂. If a modulating effect by endogenous PGD₂ is involved *in vivo*, we would assume that, in the guinea pig, it is an inhibitory influence as PGD₂ would be expected to have a relatively higher affinity to inhibitory DP₁ receptors compared with excitatory TP receptors. This is supported by our finding of a higher pIC₅₀ for PGD₂ alone compared with the lower pEC₅₀ for the excitatory effect via

the TP receptors. The more potent inhibitory effect might thus be counteracting the excitatory effect on the TP receptors, possibly explaining why the TP antagonist did not modify the dose–response curve for the inhibitory effect of PGD₂ (Figure 2). PGD₂ is rapidly metabolized through enzymic and non-enzymic processes (Fitzpatrick and Wynalda, 1983; Shibata *et al.*, 2002). Although a micromolar range of metabolite ligand concentrations was used to generate intracellular effects, some of these metabolites might be endogenous agonists on DP₂, DP₁ and TP receptors (Pettipher *et al.*, 2007). In the present study, the possibility that the enhancing effect observed at relatively high concentrations of PGD₂ and exerted via TP receptors could be due to accumulated PGD₂ metabolites in the organ bath cannot be excluded.

Mast cells were not observed in the guinea pig urinary bladder sections stained for PGDS or for DP₁ receptors. This could be due to both the perfusion of the tissue with saline and the fixative method we used in this study, as it has been reported that formalin-fixed preparations yielded much lower or no mast cell profiles compared with other fixative solutions, both in guinea pig (Ghanem *et al.*, 1988) and in human tissues (Strobel *et al.*, 1981).

In conclusion, PGD₂ can exert a dual action on contractile responses in the guinea pig detrusor muscle, with an inhibitory effect at relatively low concentrations, exerted via DP₁ receptors abundantly localized in the smooth muscle, masking an excitatory effect exerted via TP receptors. The urothelium and the suburothelium contain PGDS and therefore the necessary foundations for signalling from the urothelium to the smooth muscle are at hand. If an inhibitory influence by endogenous PGD₂ can be demonstrated and confirmed in human tissue, the role of PGD₂ would merit further studies, in relation to OAB and other disturbances in bladder function.

Acknowledgements

The authors wish to thank Dr J Bruton for help with language revision. This study was supported by the Lars Hiertas Minne Foundation, the Swedish Science Council, the Swedish National Space Board, the EU FP7 INComb and the Karolinska Institutet.

Author contributions

The study was conceived by N. N. G. and was designed by N. N. G., K. S. and L. E. G.; N. N. G. performed all organ bath experiments and N. N. G. and P. J. d. V. performed the Western blots. N. N. G. and K. S. performed the immunohistochemistry experiments which were evaluated together with L. E. G. and N. P. W.; N. N. G. compiled the data and made all the draft figures which were finalized together with L. E. G.; N. N. G. drafted the first manuscript which was revised together with L. E. G. and revised in final form and approved by all authors.

Conflict of interest

The authors have no competing interests.

References

- Abrams PH, Sykes JA, Rose AJ, Rogers AF (1979). The synthesis and release of prostaglandins by human urinary bladder muscle in vitro. *Invest Urol* 16: 346–348.
- Alexander SP, Benson HE, Faccenda E, Pawson AJ, Sharman JL, Spedding M *et al.* (2013). The Concise Guide to PHARMACOLOGY 2013/14: G protein-coupled receptors. *Br J Pharmacol* 170: 1459–1581.
- Andersson KE, Ek A, Persson CG (1977). Effects of prostaglandins on the isolated human bladder and urethra. *Acta Physiol Scand* 100: 165–171.
- Birder L, Andersson KE (2013). Urothelial signaling. *Physiol Rev* 93: 653–680.
- Birder LA, Ruggieri M, Takeda M, van Koeveinge G, Veltkamp S, Korstanje C *et al.* (2012). How does the urothelium affect bladder function in health and disease? ICI-RS 2011. *Neurourol Urodyn* 31: 293–299.
- Collins C, Klausner AP, Herrick B, Koo HP, Miner AS, Henderson SC *et al.* (2009). Potential for control of detrusor smooth muscle spontaneous rhythmic contraction by cyclooxygenase products released by interstitial cells of Cajal. *J Cell Mol Med* 13: 3236–3250.
- Davidson RA, McCloskey KD (2005). Morphology and localization of interstitial cells in the guinea pig bladder: structural relationships with smooth muscle and neurons. *J Urol* 173: 1385–1390.
- Fernandes VS, Ribeiro AS, Barahona MV, Orensanz LM, Martínez-Sáenz A, Recio P *et al.* (2013). Hydrogen sulfide mediated inhibitory neurotransmission to the pig bladder neck: role of KATP channels, sensory nerves and calcium signaling. *J Urol* 190: 746–756.
- Fitzpatrick FA, Wynalda MA (1983). Albumin-catalyzed metabolism of prostaglandin D₂. Identification of products formed in vitro. *J Biol Chem* 258: 11713–11718.
- Fry CH, Sui GP, Kanai AJ, Wu C (2007). The function of suburothelial myofibroblasts in the bladder. *Neurourol Urodyn* 26 (Suppl. 6): 914–919.
- Ghanem NS, Assem ES, Leung KB, Pearce FL (1988). Guinea pig mast cells: comparative study on morphology, fixation and staining properties. *Int Arch Allergy Appl Immunol* 85: 351–357.
- Grol S, van Koeveinge GA, de Vente J, van Kerrebroeck PE, Gillespie JI (2008). Regional differences in sensory innervation and suburothelial interstitial cells in the bladder neck and urethra. *BJU Int* 102: 870–877.
- Gronert K, Clish CB, Romano M, Serhan CN (1999). Transcellular regulation of eicosanoid biosynthesis. *Methods Mol Biol* 120: 119–144.
- Guan NN, Nilsson KF, Wiklund PN, Gustafsson LE (2014). Release and inhibitory effects of prostaglandin D₂ in guinea pig urinary bladder and the role of urothelium. *Biochim Biophys Acta* 1840: 3443–3451.
- Ishizuka O, Mattiasson A, Andersson KE (1995). Prostaglandin E₂-induced bladder hyperactivity in normal, conscious rats: involvement of tachykinins? *J Urol* 153: 2034–2038.

Jeremy JY, Tsang V, Mikhailidis DP, Rogers H, Morgan RJ, Dandona P (1987). Eicosanoid synthesis by human urinary bladder mucosa: pathological implications. *Br J Urol* 59: 36–39.

de Jongh R, Grol S, van Koeveeringe GA, van Kerrebroeck PE, de Vente J, Gillespie JI (2009). The localization of cyclo-oxygenase immuno-reactivity (COX I-IR) to the urothelium and to interstitial cells in the bladder wall. *J Cell Mol Med* 13: 3069–3081.

Kilkenny C, Browne W, Cuthill IC, Emerson M, Altman DG, Group NRRGW (2010). Animal research: reporting in vivo experiments: the ARRIVE guidelines. *Br J Pharmacol* 160: 1577–1579.

Kiriyama M, Ushikubi F, Kobayashi T, Hirata M, Sugimoto Y, Narumiya S (1997). Ligand binding specificities of the eight types and subtypes of the mouse prostanoid receptors expressed in Chinese hamster ovary cells. *Br J Pharmacol* 122: 217–224.

Larsson AK, Hagfjård A, Dahlén SE, Adner M (2011). Prostaglandin D₂ induces contractions through activation of TP receptors in peripheral lung tissue from the guinea pig. *Eur J Pharmacol* 669: 136–142.

Liu YJ, Jackson DM, Blackham A, Leff P (1996). Partial agonist effects of BW A868C, a selective DP receptor antagonist, on Cl⁻ secretion in dog tracheal epithelium. *Eur J Pharmacol* 304: 117–122.

Marcus AJ, Safier LB, Ullman HL, Islam N, Broekman MJ, Falck JR *et al.* (1987). Cell-cell interactions in the eicosanoid pathway. *Ann N Y Acad Sci* 516: 407–411.

Masick JM, Levin RM, Hass MA (2001). The effect of partial outlet obstruction on prostaglandin generation in the rabbit urinary bladder. *Prostaglandins Other Lipid Mediat* 66: 211–219.

Masunaga K, Yoshida M, Inadome A, Iwashita H, Miyamae K, Ueda S (2006). Prostaglandin E₂ release from isolated bladder strips in rats with spinal cord injury. *Int J Urol* 13: 271–276.

McGrath JC, Drummond GB, McLachlan EM, Kilkenny C, Wainwright CL (2010). Guidelines for reporting experiments involving animals: the ARRIVE guidelines. *Br J Pharmacol* 160: 1573–1576.

Munoz A, Gangitano DA, Smith CP, Boone TB, Somogyi GT (2010). Removal of urothelium affects bladder contractility and release of ATP but not release of NO in rat urinary bladder. *BMC Urol* 10: 10.

Palea S, Toson G, Pietra C, Trist DG, Artibani W, Romano O *et al.* (1998). Pharmacological characterization of thromboxane and prostanoid receptors in human isolated urinary bladder. *Br J Pharmacol* 124: 865–872.

Pawson AJ, Sharman JL, Benson HE, Faccenda E, Alexander SP, Buneman OP, Davenport AP, McGrath JC, Peters JA, Southan C, Spedding M, Yu W, Harmar AJ; NC-IUPHAR. (2014) The IUPHAR/BPS Guide to PHARMACOLOGY: an expert-driven knowledge base of drug targets and their ligands. *Nucl. Acids Res.* 42 (Database Issue): D1098–1106.

Pettipher R, Hansel TT, Armer R (2007). Antagonism of the prostaglandin D₂ receptors DP₁ and CRTH₂ as an approach to treat allergic diseases. *Nat Rev Drug Discov* 6: 313–325.

Rahnama'i MS, van Kerrebroeck PE, de Wachter SG, van Koeveeringe GA (2012). The role of prostanoids in urinary bladder physiology. *Nat Rev Urol* 9: 283–290.

Salvado MD, Alfranca A, Escolano A, Haeggström JZ, Redondo JM (2009). COX-2 limits prostanoid production in activated HUVECs and is a source of PGH₂ for transcellular metabolism to PGE₂ by tumor cells. *Arterioscler Thromb Vasc Biol* 29: 1131–1137.

Schüssler B (1990). Comparison of the mode of action of prostaglandin E₂ (PGE₂) and sulprostone, a PGE₂-derivative, on the lower urinary tract in healthy women. A urodynamic study. *Urol Res* 18: 349–352.

Shibata T, Kondo M, Osawa T, Shibata N, Kobayashi M, Uchida K (2002). 15-deoxy-delta 12,14-prostaglandin J₂. A prostaglandin D₂ metabolite generated during inflammatory processes. *J Biol Chem* 277: 10459–10466.

Strobel S, Miller HR, Ferguson A (1981). Human intestinal mucosal mast cells: evaluation of fixation and staining techniques. *J Clin Pathol* 34: 851–858.

Wheeler MA, Yoon JH, Olsson LE, Weiss RM (2001). Cyclooxygenase-2 protein and prostaglandin E₂ production are up-regulated in a rat bladder inflammation model. *Eur J Pharmacol* 417: 239–248.

Woodward DF, Jones RL, Narumiya S (2011). International Union of Basic and Clinical Pharmacology. LXXXIII: classification of prostanoid receptors, updating 15 years of progress. *Pharmacol Rev* 63: 471–538.

Supporting information

Additional Supporting Information may be found in the online version of this article at the publisher's web-site:

<http://dx.doi.org/10.1111/bph.13174>

Figure S1 Urothelium-denuded guinea pig urinary bladder strip monitored by isometric recording of muscle responses in the absence of EFS. Original experimental recording of inhibitory PGD₂ modulation of contractile responses induced by repeated applications of exogenous ATP with washings indicated by w. Tissue pretreated with diclofenac 10⁻⁶ M, repeated after each wash.

Figure S2 Cumulative dose–response curves to PGD₂, in the absence and presence of the β-adrenoceptor antagonist propranolol (10⁻⁶ M), on contractile responses in urothelium-denuded diclofenac-pretreated guinea pig urinary bladder detrusor strips evoked by electrical field stimulation (50 V, single pulses of 0.2 ms every 30 s). Data presented as mean ± SEM, *n* denotes the number of tissues, and the number of animals used for each curve was 3.

Figure S3 Fluorescence immunohistochemistry of guinea pig urinary bladder dome transmural sections showing the distribution of DP₁ and DP₂ receptors in the bladder urothelium/suburothelium and the co-localization of DP receptors with vimentin-positive profiles. To visualize interstitial cells, sections were incubated with a mouse monoclonal anti-vimentin antibody (1:500; Sigma-Aldrich, V5255). Panels A and D: sequential sections labelled with DP₁ or DP₂ antibody (green). Panels B and E: the sections in panels A and D were also immunolabelled with vimentin antibody (red). Panels C and F: superposition of staining for DP₁ or DP₂ receptors (green) and vimentin (red). Arrows in panels C and F denote interstitial cell-like profiles, showing labelling for DP₁ receptors in the cell membrane and DP₂ receptors in the cytoplasm. Symbols legend: uro denotes urothelium, sub-u denotes suburothelium, sm denotes a smooth muscle bundle, L denotes lumen.

Figure S4 Distribution of DP₂ receptors in the guinea pig urinary bladder wall and comparison with the distribution of

the neuronal marker protein PGP 9.5. Fluorescence immunohistochemistry of transmural section of male guinea pig bladder dome (A–H) as indicated. Panels A and E: immunofluorescence with DP₂ antibody (red). Panels B and F: same section, stained with antibody against PGP 9.5 (green). Panels C and G: superposition of staining for DP₂ receptors (red) and

PGP 9.5 (green). Panels D and H: combined immunofluorescence for DP₁ receptors (red), PGP 9.5 (green) and nuclear stain with H33258 (blue). Arrows in panels D and G indicate nerve-like profiles stained for PGP 9.5, uro denotes urothelium, sub-u denotes suburothelium, sm denotes smooth muscle, L denotes lumen.